Bulletin of the Seismological Society of America, Vol. 100, No. 3, pp. 1363–1369, June 2010, doi: 10.1785/0120090305

Short Note

Basement Imaging Using *Sp* Converted Phases from a Dense Strong-Motion Array in Lan-Yang Plain, Taiwan

by Chien-Hsin Chang, Ting-Li Lin, Yih-Min Wu, and Wen-Yen Chang

Abstract We have collected a large number of accelerograms recorded by the Taiwan Strong Motion Instrumentation Program (TSMIP) stations to study the thickness variations of Quaternary alluviums beneath Lan-Yang Plain, Taiwan, using an *Sp* converted wave. The estimated thicknesses of the Quaternary sediments inferred by the travel-time difference of *S* and *Sp* waves are between 200 and 1400 m and become thicker toward the northeast. In general, our resulting features of the time difference of arrivals between *Sp* and *S* waves are consistent with the previous studies on thickness variations of the Quaternary alluviums beneath Lan-Yang Plain assuming the converting point is at the unconsolidated Quaternary alluvial sediments–Miocene basement interface. Our study suggests that this technique of using *P*-*S* converted phases could be applied to the other populated basins or plains in the Taiwan region based on its dense coverage of the TSMIP stations and high seismic activity. This technique is simple and time effective and can be used to determine the general characteristics of velocity/thickness structure of a study area.

Introduction

It is well known that unconsolidated, alluvial sediments have a profound effect on the characteristics of ground shaking because of a strong impedance contrast between soft sediments and the underlying hard basement rock (Aki, 1988; Darragh and Shakal, 1991; Langston, 2003a). In addition to high values of site amplification and anelastic attenuation (Phillips and Aki, 1986; Langston, 2003b) that are commonly recognized as effects of near-surface soft, low-velocity sediments, *P*-*S* converted phases (i.e., *P*-to-*SV* or *SV*-to-*P* conversions) could be efficiently produced at a sediment–basement boundary of a strong impedance.

P-*S* converted waves have been used to map interfaces at a wide range of scale lengths. The discontinuities between lower crust and upper mantle (e.g., Moho discontinuity) and subducting lithosphere boundary have been mapped by *P*-*S* conversions (Snoke *et al.*, 1977; Ruppert *et al.*, 1998; Frederiksen *et al.*, 2003; Serrano *et al.*, 2003; Zeyen *et al.*, 2005). In the upper crust, the *P*-*S* converted phases generated at the interface between the Cenozoic unconsolidated sediments and the underlying rocks have also been studied to constrain the sediment–basement boundary (Andrews *et al.*, 1985; Chen *et al.*, 1996). Hough (1990) provided an encouraging example of using *P*-*S* conversions generated at a very shallow depth to constrain the thicknesses of low-velocity, Quaternary alluvium and Holocene mud in the San Francisco Bay area.

Lan-Yang Plain of northeastern Taiwan island is a flat, alluvial delta with an approximately equilateral triangle shape of about 30 km long at each side and located at the western terminus of the south Okinawa Trough (Fig. 1a). Lan-Yang Plain is bounded by the Hsuehshan and Central mountain ranges on its northwestern and southern sides, respectively. Inside the Lan-Yang Plain, most sediment is unconsolidated Quaternary alluvium, which is divided into two units: upper recent Holocene alluvium and lower Pleistocene clay (Chiang, 1976). According to seismic survey by the Chinese Petroleum Corporation presented in the study of Chaing (1976) and refraction survey of Wen and Yeh (1984), the unconsolidated Quaternary alluvial sediments of Lan-Yang Plain are underlain by the Miocene base complex, which has a *P*-wave velocity of 3.3–4.0 km/sec. The *P*-wave velocity of overlying recent alluvium and Pleistocene layer are of 1.4–1.7 km/sec and 1.8–2.0 km/sec, respectively. The deepest depths of recent alluvium and Pleistocene layer are about 400 and 1600 m, respectively. Figure 1c depicts the *P*-wave velocity structure of Lan-Yang Plain. The *P*-wave velocities and layer thicknesses are given in Chiang (1976) and Wen and Yeh (1984). In general, the Miocene basement tilts and the alluvium thicknesses become thicker both toward the northeast.

Furumura *et al.* (2001) observed large amplitude fundamental-mode Love waves in Lan-Yang Plain during

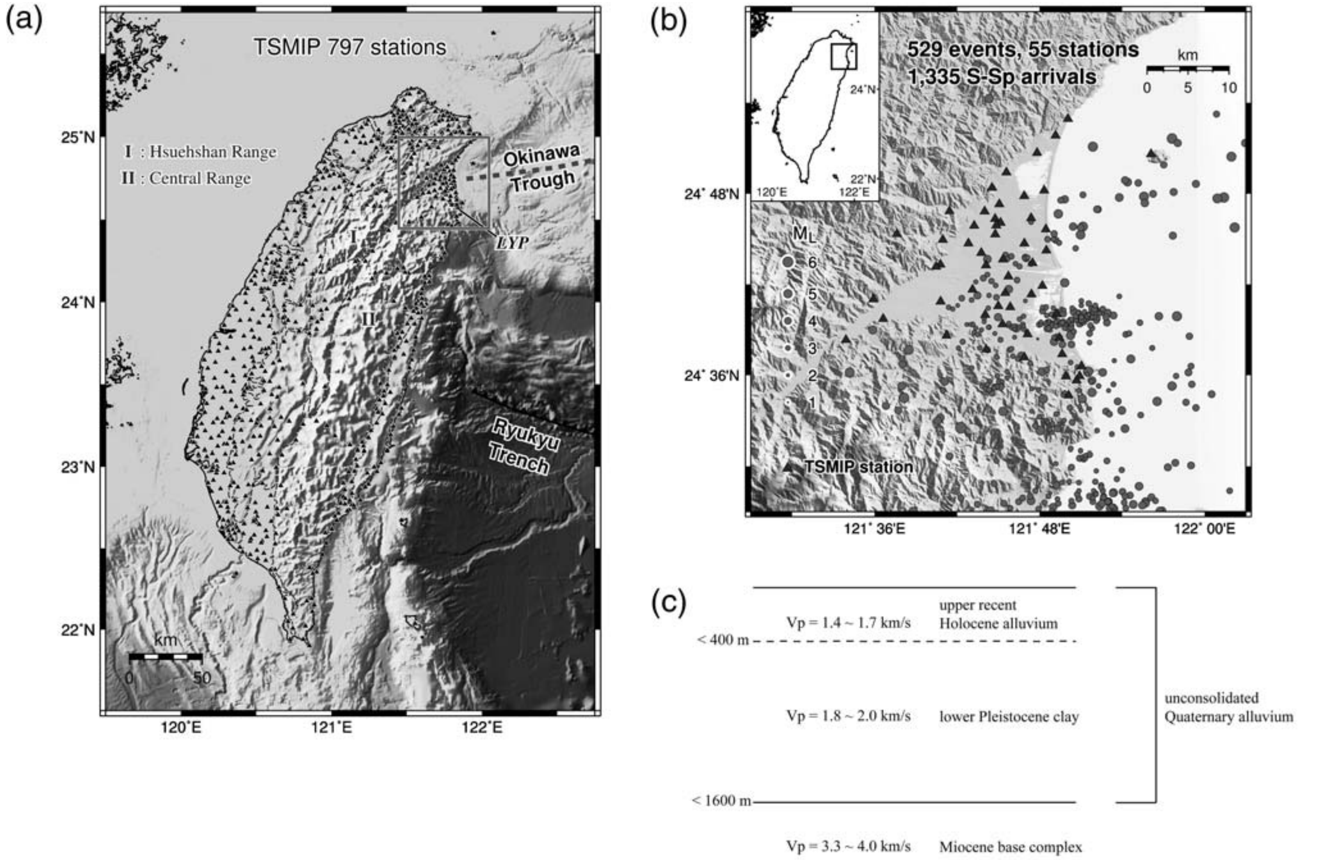

Figure 1. (a) Map showing a dense coverage of the TSMIP stations throughout the island of Taiwan. The Okinawa Trough is located northeast of the Lan-Yang Plain. The square (top right) includes the study area, Lan-Yan Plain (LYP), which is enlarged in (b). (b) Locations of the TSMIP stations and seismic events used in this study are shown by the solid triangles and circles, respectively. (c) Illustrative sketch of the *P*-wave velocity structure of Lan-Yang Plain.

the 1999 Chi-Chi earthquake. They suggested that Love waves were generated from multiple *SH*-wave reflections between the free-surface and sediment–basement interface; in other words, the hard basement creates an effective bounded environment to the overlying alluvial sediments in Lan-Yang Plain. Based on the velocity contrasts between Quaternary alluvium and Miocene basement and Love-wave generation observed and modeled in the study by Furumura *et al.* (2001), our working hypothesis for this study is that *P*-*S* converted phases are started from *P* and *SV* waves interacting with the interface between unconsolidated Quaternary alluvial sediments and Miocene basement but not with the other deeper or shallower seismic impedance boundaries. Besides the favorable factors of velocity structure setting for generating *P*-*S* converted wave, Lan-Yang Plain in northeastern Taiwan is situated on a high seismicity region, which provided abundant local seismic events that have been carefully chosen in this study. *P*-*S* converted phases are commonly observed at the Taiwan Strong Motion Instrumentation Program (TSMIP) stations within Lan-Yang Plain. Figure 2a and b show a simple illustration of *P*-*S* converted phases and an example of typical *S*-to-*P* converted phase (*Sp*) recorded at an TSMIP station within Lan-Yang Plain from a local earthquake.

The main objective of this study is to use travel-time differences between direct *S* waves and converted *Sp* waves to infer the thickness variations of the unconsolidated Quaternary alluvial sediments beneath Lan-Yang Plain. We will show that our resulting distribution of the time difference of arrivals between *S* and *Sp* waves is consistent with the thickness contours of Quaternary sediments at Lan-Yang Plain from large-scale seismic refraction/reflection surveys (Chaing, 1976).

Data Acquisition and Analysis

We used the accelerograms from local earthquakes recorded by the TSMIP (Shin, 1993; Liu *et al.*, 1999) strong-motion stations situated on Lan-Yang Plain (Fig. 1b). TSMIP, operated by the Taiwan Central Weather Bureau (CWB), consists of over 800 strong-motion stations as of 2008 located throughout the Taiwan island and has being recording earthquake strong motions since 1992. The TSMIP stations are equipped with three-component, force-balance

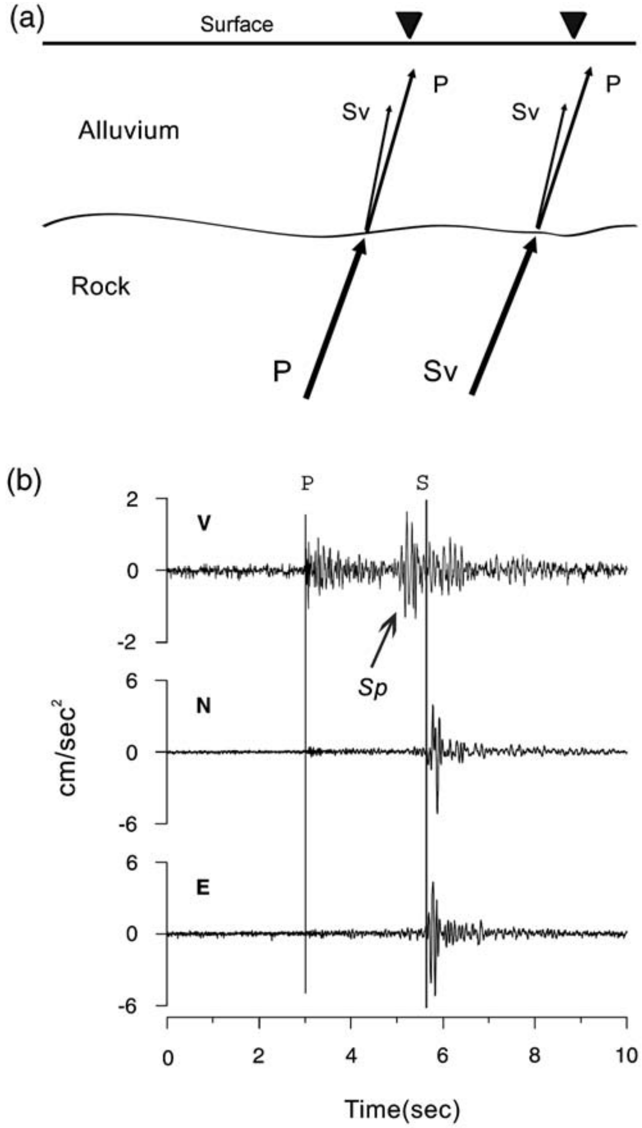

Figure 2. (a) Simple illustration of *P*-*S* converted phases and (b) example of a typical *S*-to-*P* converted phase (*Sp*) recorded at an TSMIP station within Lan-Yang Plain from a local earthquake.

accelerometers with a 16 or 24 bit resolution digitizer at a sampling rate of 200 Hz or higher. The instrument acceleration response of each station is flat from direct current to about 50 Hz.

We collected the seismic events between 1993 and 2007 that were located in the northeastern Taiwan region and recorded by the TSMIP stations of Lan-Yang Plain. In general, the earthquake catalog in Taiwan is provided by the Central Weather Bureau Seismic Network (CWBSN). The earthquake locations used in this study were relocated using 3D V_P and V_P/V_S models (Wu *et al.*, 2007, 2008; Wu, Shyu, *et al.*, 2009; Wu, Zhao, *et al.*, 2009) and incorporating the CWBSN, TSMIP, and Japan Meteorological Agency stations. In total, about 900 stations were used for earthquake relocation. The 3D location method of Thurber and Eberhart-Phillips (1999) was used in this study, in which theoretical travel times of *P* and *S* waves are calculated by 3D ray tracing (Thurber, 1993). On the other hand, the CWBSN earthquake catalog only uses CWBSN stations (about 90 stations) and the 1D velocity model of Chen (1995). As a result, the relocated earthquake catalog has been proven to yield a better constraint on earthquake location than the CWBSN earthquake catalog (Wu *et al.*, 2008). More precise earthquake locations are needed to better define the geometric relation between stations and earthquakes, which in turn, will enable us to better select a local earthquake having more vertically propagating waves interacting with the Quaternary sediments of Lan-Yang Plain.

In this study, we only considered the local earthquakes that had not traveled rather long distances, which might complicate *P* and *S* arrivals. In order to confine *P* and *S* waves to those polarized on the vertical and horizontal components, respectively, we chose local earthquakes that have a takeoff angle greater than 150° and a focus depth deeper than 6 km. These criteria on takeoff angle and focus depth are based on an attempt to better conform vertical incidence of local propagating body waves when crossing the sediment–basement interface. We calculated the takeoff angle by simply connecting an earthquake focus and a recording station with a straight line, and from this we defined the takeoff angle as the angle rotating clockwise from the down vertical to the connecting line. In our study we used the *Sp* converted phase instead of *Ps* (*P*-to-*S*) phase. Because a sediment–basement interface is very close to the ground surface compared to the Moho discontinuity, a *Ps* wave is more prone to be affected by the source rupture duration or contaminated by a *P* coda than an *Sp* wave. Therefore, an *Sp* wave is more distinct and observable than a *Ps* wave where a converting point is shallow, such as at a base of unconsolidated embayment (Andrews *et al.*, 1985; Chen *et al.*, 1996; Langston, 2003a). The *Sp* phase from a single, smooth interface with an abrupt velocity contrast of a local earthquake should be simple and be similar to the *P*-wave or *S*-wave pulse.

After applying the previous selection criteria on takeoff angle and focus depth of the relocated local earthquakes between 1993 and 2007, there are a total 529 events recorded by 55 TSMIP stations at Lan-Yang Plain and 1335 manually picked time differences of $S - Sp$ arrivals. Among the 55 TSMIP stations that provided recordings of the events, 11 stations provided less than 10 records of time difference of $S - Sp$ arrivals and were not used in our study (Fig. 1b).

Results

Table 1 lists the information on locations of the TSMIP stations and seismic events and event numbers, mean $S - Sp$ travel-time differences, and their corresponding standard deviations for each of the 44 TSMIP stations. The spatial distribution of the resulting time differences of $S - Sp$ arrivals is plotted in Figure 3a. Note that the general pattern of spatial distribution shown in Figure 3a will not change whether the 11 stations that provided less than 10 records are used or not.

Table 1
Locations of TSMIP Stations and $S-Sp$ Time Differences

Number	Station Code	Longitude (°E)	Latitude (°N)	Number of Records	Mean $S-Sp$ (sec)	Standard Deviation
1	ILA001	121.8348	24.8827	10	0.788	0.163
2	ILA002	121.7972	24.8452	12	0.857	0.243
3	ILA003	121.7817	24.7977	23	0.859	0.169
4	ILA004	121.7818	24.7453	42	1.216	0.213
5	ILA005	121.8037	24.6987	36	0.911	0.159
6	ILA006	121.8245	24.6413	50	0.642	0.147
7	ILA007	121.8453	24.5943	49	0.509	0.144
8	ILA008	121.7625	24.7090	55	0.862	0.205
9	ILA010	121.7818	24.6197	26	0.442	0.133
10	ILA012	121.7337	24.7807	14	0.627	0.245
11	ILA013	121.7295	24.7350	28	0.836	0.211
12	ILA014	121.7190	24.6945	37	0.720	0.152
13	ILA016	121.6830	24.7495	10	0.626	0.168
14	ILA018	121.6802	24.6813	20	0.556	0.109
15	ILA019	121.6873	24.6437	15	0.620	0.130
16	ILA025	121.5655	24.6390	13	0.768	0.158
17	ILA026	121.7647	24.6752	24	0.909	0.176
18	ILA027	121.7587	24.6908	55	0.888	0.105
19	ILA028	121.7465	24.7555	29	1.042	0.124
20	ILA029	121.7463	24.7725	11	0.957	0.153
21	ILA030	121.7560	24.7278	39	1.080	0.152
22	ILA031	121.8323	24.5988	44	0.657	0.137
23	ILA032	121.8277	24.6233	40	0.606	0.105
24	ILA034	121.8058	24.8038	12	1.013	0.117
25	ILA036	121.7515	24.7887	17	0.752	0.147
26	ILA038	121.7353	24.7212	48	0.931	0.164
27	ILA039	121.7210	24.7650	16	0.848	0.186
28	ILA040	121.7900	24.7733	16	1.140	0.203
29	ILA041	121.7917	24.7238	46	1.022	0.107
30	ILA042	121.7905	24.6893	48	0.972	0.093
31	ILA043	121.7355	24.6285	16	0.995	0.279
32	ILA044	121.7553	24.6563	28	0.800	0.128
33	ILA046	121.7343	24.6667	50	0.613	0.082
34	ILA047	121.7858	24.6453	47	0.662	0.116
35	ILA048	121.7530	24.7682	26	1.014	0.169
36	ILA049	121.7478	24.7653	24	0.943	0.173
37	ILA051	121.6747	24.7198	15	0.792	0.140
38	ILA052	121.8512	24.6100	28	0.553	0.121
39	ILA055	121.8085	24.7377	20	1.127	0.196
40	ILA056	121.8080	24.7610	23	1.223	0.237
41	ILA058	121.7502	24.6763	48	0.865	0.151
42	ILA059	121.8212	24.6673	39	0.849	0.162
43	ILA060	121.8357	24.5777	14	0.427	0.101
44	ILA068	121.8490	24.5990	13	0.399	0.143

In order to justify the spatial distribution shown in Figure 3a, we compared it with the thickness contour of the Quaternary sediments beneath Lan-Yang Plain (Chiang, 1976) in Figure 3b based on a working hypothesis that the Sp-converted phase is started at the Pleistocene sediments–Miocene basement boundary from nearly vertically incident SV waves. Figure 3b shows that the boundary between the Pleistocene sediments–Miocene basement has a basinlike shape with a deepest section around the western side of the Kueishantao Sea area of about 1600 m and that the thicknesses of the overlying Quaternary sediments become thicker toward the northeast. Comparisons between Figure 3a and b show that the spatial distribution of the time differences of $S-Sp$ arrivals are consistent with the general features of the thickness contour of the Quaternary sediments implying that thicker Quaternary sediments correspond to a larger $S-Sp$ travel-time difference.

The time difference of $S-Sp$ arrivals can be related to the layer thickness in a single, flat layer model (Fig. 2a) from a vertically incident wave by

$$H = [V_P/(V_P/V_S - 1)]dt_{S-Sp}, \tag{1}$$

where H is the depth to the wave converting point, V_P and V_S are the average P- and S-wave velocities of the layer, and dt_{S-Sp} is the $S-Sp$ travel-time difference. Brocher (2005)

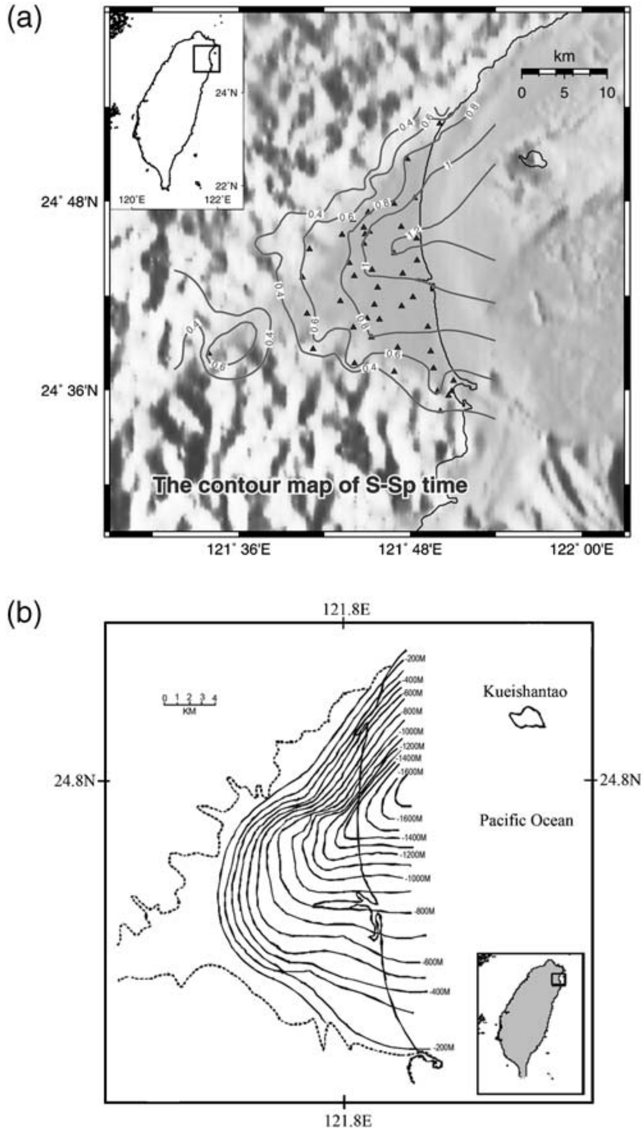

Figure 3. (a) Spatial distribution of the observed time differences of $S - Sp$ arrivals. The triangles show the 44 TSMIP stations contributing to the spatial distribution. The time differences are in units of seconds. (b) The contour of thickness for the Quaternary alluvial sediments in Lan-Yang Plain. The contour map is modified from Chiang (1976). The contours are in units of meters.

presented empirical relations among V_P, V_S, and density for the Earth's crust. He proposed the Brocher's empirical fit equation (equation 11 in Brocher, 2005) to empirically estimate Poisson's Ratio (i.e., V_P/V_S ratio) as a function of V_P, which is valid for typical V_P values of Quaternary alluvium lying between 1.5 and 3.0 km/sec. Therefore, one can assign V_P and dt_{S-Sp} values and then get an H value using equation (1) through application of the Brocher's empirical fit equation to find the V_P/V_S ratio first. The V_P/V_S structure beneath Taiwan obtained in Wu *et al.* (2007) by seismic tomography has a shallowest grid point at a depth of 2 km, which is greater than the expected thickness of the unconsolidated Quaternary alluvium at Lan-Yang Plain.

Figure 4 plots the Quaternary alluvium thickness at Lan-Yang Plain as a function of V_P and dt_{S-Sp}. For the TSMIP stations located at the northeastern location of Lan-Yang Plain with a dt_{S-Sp} of about 1.2 sec (Fig. 3a), we found that an average V_P of about 2.0 km/sec will give an adequate estimation of the sediment thickness (Fig. 4a) comparable to that obtained in Chiang (1976). Around the western and southern sides of the boundary of Lan-Yang Plain, a dt_{S-Sp} of 0.6 sec yields comparable sediment thicknesses of about 200–400 m (Chiang, 1976) giving an average V_P of about 1.65–1.8 km/sec (Fig. 4b). A slower average V_P around the boundary than that of the northeastern of Lan-Yang Plain is qualitatively explained by the thinning of the Pleistocene alluvium toward the edge of Lan-Yang Plain and the northeastward thickening of the Pleistocene alluvium, which has a slightly faster P-wave velocity than the overlying recent Holocene alluvium. The estimated thicknesses of the Quaternary sediments beneath Lan-Yang Plain inferred by the travel-time difference of S and Sp waves are overall between 200 and 1400 m and are in agreement on that of Chiang (1976).

The standard deviations of $S - Sp$ travel-time difference (Table 1) could arise from a variety of sources such as

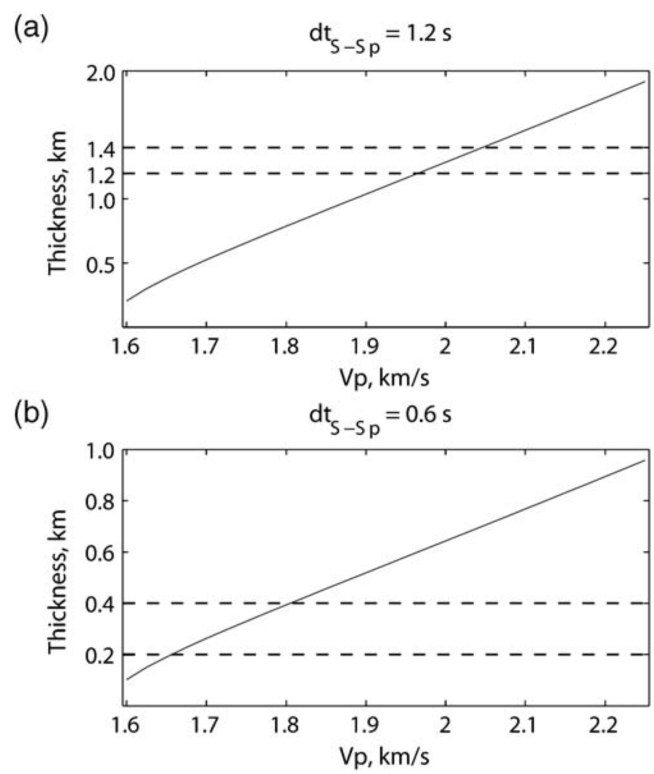

Figure 4. Realizations of equation (1) for two different $S - Sp$ travel-time differences (dt_{S-Sp}). Sediment thickness is expressed as a function of P-wave velocity. (a) For $dt_{S-Sp} = 1.2$ sec given in Figure 3a, the corresponding thickness of the Quaternary alluvial sediment is 1.2–1.4 km, as indicated in Figure 3b and reflects an average P-wave velocity of the sediments of about 2.0 km/sec. (b) For $dt_{S-Sp} = 0.6$ sec, the inferred average P-wave velocity of the sediments is about 1.75 km/sec.

seismic noise, picking uncertainty, and thickness/velocity variations beneath each station, etc. In general, the standard deviation decreases as the number of recordings increases (Fig. 5a) suggesting canceling of seismic noise or picking uncertainty. Stations ILA004 and ILA008 are two notable exceptions in Figure 5a that both show large values of recording numbers and standard deviation implying site structure variations or strong background noise at these two stations. Undoubtedly, a more detailed investigation is needed to support our conclusions. Figure 5b shows the spatial distribution of the standard deviation and does not show prominent localization or patterns.

Conclusion

A large number of high-quality accelerograms were collected by TSMIP strong-motion stations of Lan-Yang Plain from numerous local earthquakes occurring between 1993 and 2007 to estimate the thickness of Quaternary alluvium beneath Lan-Yang Plain using *Sp* converted waves. In general, the resulting features of the time difference of arrivals between *Sp* and *S* waves and their inferred thicknesses are consistent with thickness variations of the Quaternary alluvium beneath Lan-Yang Plain obtained in Chaing (1976) and Wen and Yeh (1984) by seismic reflection/refraction measurements. Therefore, commonly observed *P*-*S* converted waves at the TSMIP stations of Lan-Yang Plain are likely started with propagating *P* and *S* waves interacting with the Pleistocene sediments–Miocene basement interface. Such a sediment–basement interface might have important implications for earthquake hazard assessments such as generation of multiple *SH*-wave reflections as observed in Furumura *et al.* (2001).

We have presented a first attempt on using *Sp* converted phase from a dense strong-motion array (TSMIP) in Taiwan to investigate the thickness variations of an alluvial plain, Lan-Yang Plain. Our study implies that a dense coverage of the TSMIP stations and high seismic activity throughout the Taiwan region could serve to provide high-quality and high-quantity *P*-*S* converted waves to study sediment thickness or velocity structure for the other populated areas situated on a basin or plain such as Chianan Plain, Pingtung Plain, or Taipei Basin in Taiwan or the other similar places around the world. This technique of using an *Sp* converted phase is simple and time-effective and can be used to preliminarily define the general characteristics of velocity/thickness structure for a region with available converted phases before conducting comprehensive onsite geophysical surveys.

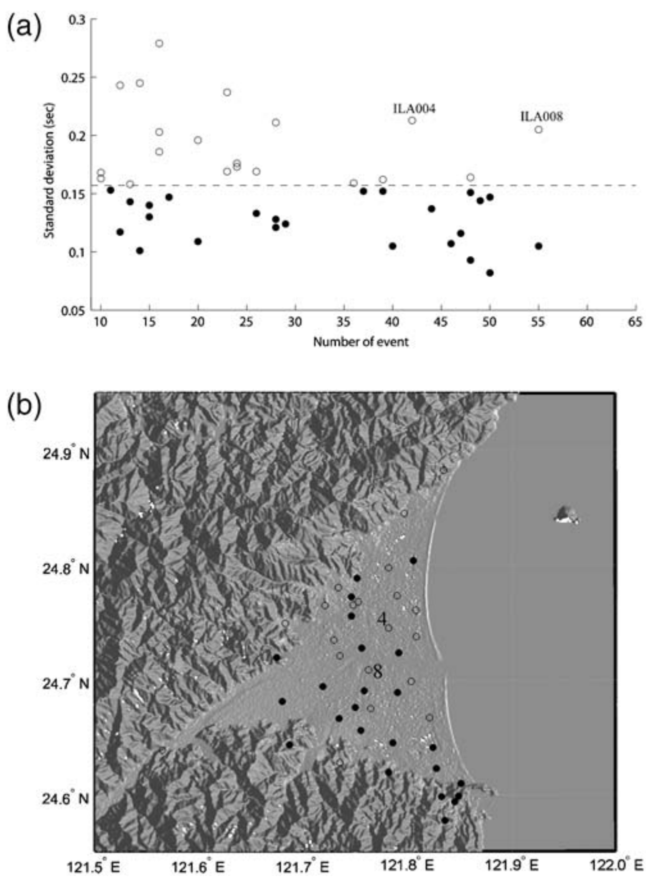

Figure 5. (a) Relation between the standard deviation and the number of events recorded. The dashed line indicates the average of the standard deviation. Solid and open circles represent smaller and larger standard deviations than the average, respectively. (b) Spatial distribution of the standard deviation. Numbers 4 and 8 represent TSMIP stations ILA004 and ILA008, respectively. Solid and open circles have the same representation as in (a).

Data and Resources

Raw accelerograms can be obtained upon request to the Central Weather Bureau of the Republic of China or to C.-H. Chang. The software package GMT (Wessel and Smith, 1998) was used in this study and is gratefully acknowledged.

Acknowledgments

This work was supported by the National Science Council and the Central Weather Bureau of the Republic of China. We thank our one anonymous reviewer and Diane Doser, the Associate Editor, for their valuable and constructive comments.

References

Aki, K. (1988). Local site effects on strong ground motion, in *Earthquake Engineering and Soil Dynamics II: Recent Advances in Ground-Motion Evaluation* J. L. V. Thun (Editor), American Society of Civil Engineers, Park City, Utah, 103–155.

Andrews, M. C., W. D. Mooney, and R. P. Meyer (1985). The relocation of microearthquakes in the northern Mississippi embayment, *J. Geophys. Res.* **90,** 10,223–10,236.

Brocher, T. M. (2005). Empirical relations between elastic wavespeeds and density in the Earth's crust, *Bull. Seismol. Soc. Am.* **95,** 2081–2092, doi 10.1785/0120050077.

Chen, Y. L. (1995). A study of 3-D velocity structure of the crust and the subduction zone in the Taiwan region, *Master's Thesis*, National Central University, Chungli City, Taiwan, 1972 pp. (in Chinese).

Chen, K., J. Chiu, and Y. Yang (1996). Shear-wave velocity of the sedimentary basin in the upper Mississippi embayment using *S*-to-*P* converted waves, *Bull. Seismol. Soc. Am.* **86,** 848–856.

Chiang, S. C. (1976). A seismic refraction prospecting of the Ilan plain, *Minging Tech.* **14,** 215–221.

Darragh, R. B., and A. F. Shakal (1991). The site response of two rock and soil station pairs to strong and weak ground motion, *Bull. Seismol. Soc. Am.* **81,** 1885–1899.

Frederiksen, A. W., H. Folsom, and G. Zandt (2003). Neighbourhood inversion of teleseismic *Ps* conversions for anisotropy and layer dip, *Geophys. J. Int.* **155,** 200–212.

Furumura, M., T. Furumura, and K.-L. Wen (2001). Numerical simulation of Love wave generation in the Ilan Basin, Taiwan, during the 1999 Chi-Chi earthquake, *Geophys. Res. Lett.* **28,** 3385–3388.

Hough, S. E. (1990). Constraining sediment thickness in the San Francisco Bay area using observed resonances and *Ps* conversions, *Geophys. Res. Lett.* **17,** 1469–1472.

Langston, C. A. (2003a). Local earthquake wave propagation through Mississippi embayment sediments, part I: Body-wave phases and local site responses, *Bull. Seismol. Soc. Am.* **93,** 2664–2684.

Langston, C. A. (2003b). Local earthquake wave propagation through Mississippi embayment sediments, part II: Influence of local site velocity structure on Q_p and Q_s determinations, *Bull. Seismol. Soc. Am.* **93,** 2685–2702.

Liu, K. S., T. C. Shin, and Y. B. Tsai (1999). A free-field strong motion network in Taiwan: TSMIP, *Terr. Atmos. Ocean. Sci.* **10,** 377–396.

Phillips, W. S., and K. Aki (1986). Site amplification of coda waves from local earthquakes in central California, *Bull. Seismol. Soc. Am.* **76,** 627–648.

Ruppert, S., M. M. Fliedner, and G. Zandt (1998). Thin crust and active upper mantle beneath Southern Sierra Nevada, *Tectonophysics* **286,** 237–252.

Serrano, I., D. Zhao, J. Morales, and F. Torcal (2003). Seismic tomography from local crustal earthquakes beneath eastern Rif Mountains of Morocco, *Tectonophysics* **367,** 187–201.

Shin, T. C. (1993). Progress summary of the Taiwan strong-motion instrumentation program, in *Symposium on the Taiwan Strong-Motion Program*, Taipei, Taiwan, 28–29 December, 1–10.

Snoke, J. A., I. S. Sacks, and H. Okada (1977). Determination of the subducting lithosphere boundary by use of converted phases, *Bull. Seismol. Soc. Am.* **67,** 1051–1060.

Thurber, C. H. (1993). Local earthquake tomography: Velocities and V_P/V_S—theory, in *Seismic Tomography: Theory and Practice* H. M. Iyer and K. Hirahara (Editors), Chapman and Hall, London, 563–583.

Thurber, C., and D. Eberhart-Phillips (1999). Local earthquake tomography with flexible gridding, *Comput. Geosci.* **25,** 809–818.

Wen, K.-L., and Y.-T. Yeh (1984). Seismic velocity structure beneath the SMART-1 array, *Bull. Inst. Earth Sci. Acad. Sin.* **4,** 51–72.

Wessel, P., and W. H. F. Smith (1998). New, improved version of Generic Mapping Tools released, *Eos Trans. Am. Geophys. Union* **79,** 579.

Wu, Y. M., C. H. Chang, L. Zhao, J. B. H. Shyu, Y. G. Chen, K. Sieh, and J. P. Avouac (2007). Seismic tomography of Taiwan: Improved constraints from a dense network of strong-motion stations, *J. Geophys. Res.* **112,** B08312, doi 10.1029/2007JB004983.

Wu, Y. M., C. H. Chang, L. Zhao, T. L. Teng, and M. Nakamura (2008). A comprehensive relocation of earthquakes in Taiwan from 1991 to 2005, *Bull. Seismol. Soc. Am.* **98,** 1471–1481.

Wu, Y. M., J. B. H. Shyu, C. H. Chang, L. Zhao, M. Nakamura, and S. K. Hsu (2009). Improved seismic tomography offshore northeastern Taiwan: Implications for subduction and collision processes between Taiwan and the southernmost Ryukyu, *Geophys. J. Int.* **178,** 1042–1054, doi 10.1111/j.1365-246X.2009.04180.x.

Wu, Y. M., L. Zhao, C. H. Chang, N. C. Hsiao, Y. G. Chen, and S. K. Hsu (2009). Relocation of the 2006 Pingtung earthquake sequence and seismotectonics in Southern Taiwan, *Tectonophysics* **479,** 19–27.

Zeyen, H., P. Ayarza, M. Fernandez, and A. Rimi (2005). Lithospheric structure under the western African–European plate boundary: A transect across the Atlas Mountains and the Gulf of Cadiz, *Tectonics* **24,** 1–16.

Central Weather Bureau
Taipei 100, Taiwan
gensin@scman.cwb.gov.tw
(C.-H.C.)

Department of Geosciences
National Taiwan University
Taipei 10617, Taiwan
tinglilin@ntu.edu.tw
drymwu@ntu.edu.tw
(T.-L.L., Y.-M.W.)

Department of Natural Sciences
National Science Council
Taiwan
wychang@nsc.gov.tw
(W.-Y.C.)

Manuscript received 18 September 2009